*Journal of Microscopy, Vol. 213, Pt 1 January 2004, pp. 1–5*
*Received 20 March 2003; accepted 4 September 2003*

SHORT COMMUNICATION

# Graphical representation and multicomponent analysis of single-frequency fluorescence lifetime imaging microscopy data

A. H. A. CLAYTON*, Q. S. HANLEY† & P. J. VERVEER‡
*Ludwig Institute for Cancer Research, PO Box 2008, Royal Melbourne Hospital, Parkville, Victoria 3050, Australia
†Department of Biological and Chemical Sciences, University of the West Indies, Cave Hill Campus, St. Michael, Barbados
‡Cell Biology and Cell Biophysics Program, European Molecular Biology Laboratory, Meyerhofstraße 1, D-69117 Heidelberg, Germany

**Key words.** Epidermal growth factor receptor, fluorescence lifetime imaging microscopy (FLIM), fluorescence resonance energy transfer (FRET), green fluorescent protein (GFP), phosphorylation, protein interactions, two-component analysis.

## Summary

Graphical representation of fluorescence lifetime imaging microscopy data demonstrates that a mixture of two components with single exponential decays can be resolved by single frequency measurements. We derive a method based on linear fitting that allows the calculation of the fluorescence lifetimes of the two components. We show that introduction of proper error-weighting results in a non-linear method that is mathematically identical to a global analysis algorithm that was recently derived. The graphical approach was applied to cellular data obtained from a lifetime-based phosphorylation assay for the epidermal growth factor receptor and yielded results similar to those obtained by a global analysis algorithm.

## Introduction

Fluorescence lifetime imaging microscopy (FLIM) in the frequency domain (Lakowicz & Berndt, 1991; Gadella *et al.*, 1993) has proven to be a valuable tool to resolve spatially the fluorescence lifetimes of one or more probes, for instance to monitor fluorescence resonance energy transfer (FRET) in intact cells (Bastiaens & Squire, 1999; Wouters *et al.*, 2001). In a recent publication, the ability to resolve two lifetimes using measurements at a single frequency was investigated, and an efficient global analysis algorithm was proposed that is capable of resolving the molar fractions of two components providing that their lifetimes are spatially invariant in the sample (Verveer & Bastiaens, 2003).

Traditionally, single-frequency FLIM data have been analysed and represented in terms of phase and modulation lifetimes that are useful for a semiquantitative description of the fluorophore environment (Gadella *et al.*, 1994). However, even in the apparently simple situation of a population distribution between two fluorescence lifetime species, the phase and modulation lifetimes are non-linear functions of the component populations. Multicomponent analysis of single-frequency spectroscopic data has been treated by Weber (1981). Gadella *et al.* (1994) have also presented two-component analysis of single frequency data when one of the two lifetimes is known *a priori*. In this communication, we present an alternative graphical analysis method as a means of visualizing and analysing FLIM data in terms of two-component models. Here we transform the measured phases and modulations so they become linear functions of the populations of species, an approach that was used before in the development of global analysis algorithms for frequency domain FLIM data (Verveer *et al.*, 2000a; Verveer & Bastiaens, 2003). This methodology is similar to other approaches including analysis of two-state binding isotherms (Hirshfield *et al.*, 1993) and the subtraction of background fluorescence in phase-modulation spectroscopy (Lakowicz *et al.*, 1987). More recently, it has found application in the analysis of excited-state decay kinetics obtained by time-domain spectroscopy (Itagaki *et al.*, 1997). We test the graphical representation analysis on cellular FLIM data, compare the results of the graphical analysis method to global analysis algorithms developed recently and discuss possible extensions of the technique to more complex situations.

Correspondence to: Dr Peter J Verveer. Fax: +49 622 138 7306; e-mail: peter.verveer@embl-heidelberg.de

### Graphical analysis of FLIM data

The present work is closely related to previous work by Verveer & Bastiaens (2003) and therefore follows the notation therein. We start by transforming the measured phase $\varphi_i$ and modulation $M_i$:

$$A_i = M_i \sin(\varphi_i) = \frac{\alpha_i \omega\tau_1}{1+\omega^2\tau_1^2} + \frac{(1-\alpha_i)\omega\tau_2}{1+\omega^2\tau_2^2}, \quad (1a)$$

$$B_i = M_i \cos(\varphi_i) = \frac{\alpha_i}{1+\omega^2\tau_1^2} + \frac{1-\alpha_i}{1+\omega^2\tau_2^2}. \quad (1b)$$

The subscript $i$ refers to the $i$th pixel in a microscope image, $\omega = 2\pi f$ is the circular frequency corresponding to the frequency $f$, $\omega\tau_1$ is the spatially invariant frequency-lifetime product for component one, $\omega\tau_2$ the analogous quantity for component two, $\alpha_i$ is the spatially dependent fraction of the fluorescence emitted by component one, and $(1 - \alpha_i)$ is the fluorescent fraction of component two. Molar fractions of the components can be found from the fluorescent fractions by renormalization with the quantum yields of the components, which, in the case of FRET, is equivalent to renormalization with their lifetimes (Verveer *et al.*, 2001a). Figure 1(a) shows a plot of $A$ vs. $B$ for $\alpha_i = 1$ (one-component model) as a function of $\omega\tau_1$, and plots for three spatially dependent mixtures (two-component model) with spatially invariant lifetimes as a function of $\alpha$, as predicted by Eq. (1). The half-circle going through the points (0, 0) (1, 0) and ($^1/_2$, $^1/_2$) represents all possible spatially invariant one-component lifetime models measured at a frequency of 80 MHz. Line segments connecting two positions on the half-circle give all possible values for spatially dependent mixtures of two components with spatially invariant lifetimes determined by the two points on the half-circle. Three examples of this are shown for different lifetime pairs at a frequency of 80 MHz.

From the plot of the ($A_i$, $B_i$) pairs we can extract the lifetimes of the individual components by finding the intersections of a straight line through the data points with the half-circle of single-component values. We focus here only on the estimation of the two lifetimes, because calculating the populations is then reduced to a simple linear estimation, for which an equation has previously been derived (Verveer & Bastiaens, 2003). First we derive expressions for the offset $u$ and slope $v$ of the straight line $A_i = u + vB_i$:

$$u = \frac{1}{\omega(\tau_1+\tau_2)} \text{ and } v = \frac{\omega\tau_1\tau_2 - 1}{\omega(\tau_1+\tau_2)}. \quad (2)$$

If the offset $u$ and slope $v$ of the straight line are known, the two lifetimes can be directly calculated:

$$\tau_{1,2} = \frac{1 \pm \sqrt{1-4u(u+v)}}{2\omega u}. \quad (3)$$

Thus, one strategy to find the two lifetimes, given a set of ($A_i$, $B_i$) pairs, is to fit a straight line to a plot of $A_i$ vs. $B_i$ and then

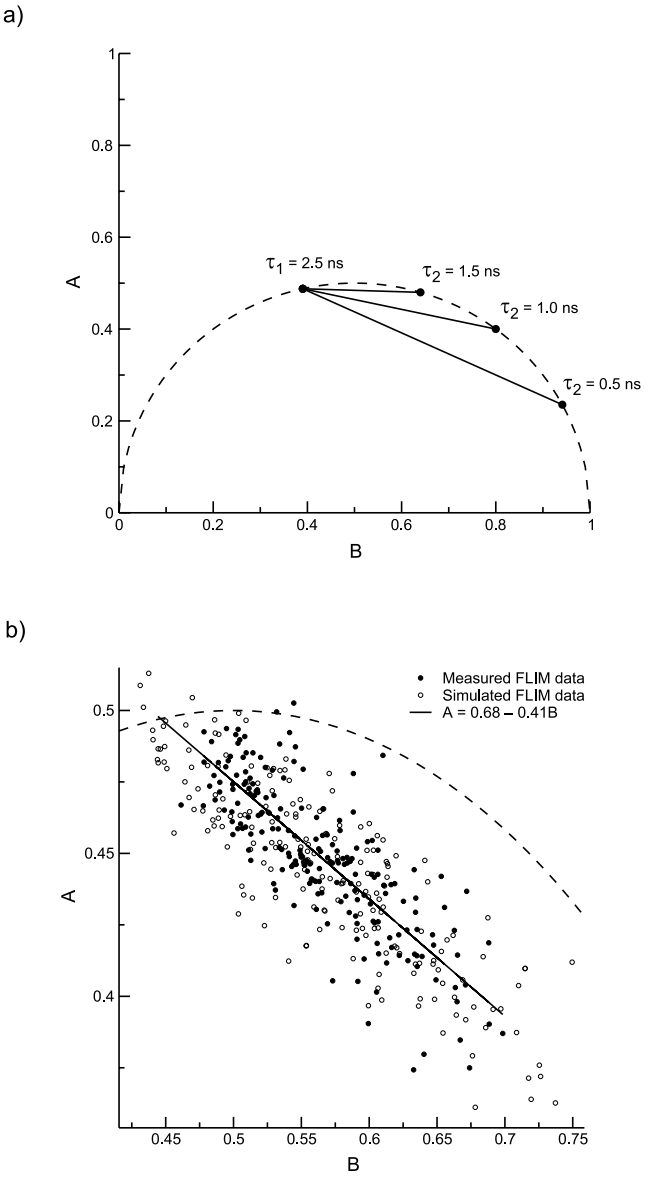


**Fig. 1.** (a) Plot of $A$ vs. $B$ for one- and two-component mixtures. The half circle represents all possible ($A$, $B$) pairs for single-exponential decays (one-component model) from $\tau = 0$ (0, 0) to $\tau = \infty$ (1, 0). Shown also are the possible ($A$, $B$) values for three different mixtures from $\alpha = 0$ to $\alpha = 1$, each with a longer lifetime of 2.5 ns, and with shorter lifetimes of 1.5, 1.0 or 0.5 ns, respectively, for measurements at 80 MHz. (b) Plot of ($A_i$, $B_i$) pairs from FLIM data measured at 80.06 MHz, of cells expressing EGFR-GFP (closed circles, see text for details). Shown also is the straight line found by linear regression to the data. The fitted parameters were: $u = 0.68$, $w = 0.41$. The lifetimes found by the linear fitting approach were: $\tau_1 = 2.23$, $\tau_2 = 0.72$ ns, and lifetimes derived from a non-linear error-weighted fit were $\tau_1 = 2.22$, $\tau_2 = 0.69$ ns. Also shown are simulated data points for a two-component model with single-exponential decays with lifetimes equal to 2.23 and 0.72 ns (open circles, see text for details).

calculate the lifetimes with Eq. (3). This approach is attractive because a linear fit can be implemented relatively easily in a speed- and memory-efficient way, even for large data sets.

Real data contain noise, and any rigorous analysis must use some form of error weighting. Error estimates $\sigma_{A,i}$ and $\sigma_{B,i}$ can be found (Verveer *et al.*, 2001a), but because both $A_i$ and $B_i$ have errors, standard linear fitting methods that assume that the independent variable is noise free are not applicable. One solution to this problem uses minimization of a $\chi^2$ merit function of the form:

$$\chi^2(u,v) = \sum_i \frac{(A_i - u - vB_i)^2}{\sigma_{A,i}^2 + v^2\sigma_{B,i}^2}, \qquad (4)$$

where the weighting factor in the denominator follows from the variance of a linear combination of two random variables: $\mathrm{Var}(A_i - u - vB_i) = \mathrm{Var}(A_i) + v^2\mathrm{Var}(B_i)$ (Press *et al.*, 1992). This merit function is not linear in $u$ and $v$, and therefore a non-linear minimization approach must be used to find $u$ and $v$. Instead of minimizing Eq. (4) and then applying Eq. (3) we may also first substitute Eq. 2 into the merit function (Eq. 4) and directly minimize for $\tau_1$ and $\tau_2$. We then find a second merit function that is the same as derived more directly by Verveer & Bastiaens (2003):

$$\chi^2(u,v) = \sum_i \frac{((\omega^2\tau_1\tau_2 - 1)B_i - \omega(\tau_1 + \tau_2)A_i + 1)^2}{\omega^2(\tau_1 + \tau_2)^2\sigma_{A,i}^2 + (\omega^2\tau_1\tau_2 - 1)\sigma_{B,i}^2}. \qquad (5)$$

These two approaches are fully equivalent, although minimization of Eq. (4) may make use of its partial linear nature (Press *et al.*, 1992). In practice, we find minimization of Eq. (5) with a standard minimization routine the most convenient.

For most of our data we prefer an error-weighted fit to a linear fit without errors, because it avoids possible problems with noisy data. However, the linear approach introduced here has its merits because a linear fit is easily implemented and is computationally efficient. Some form of approximate error weighting may still be used, for instance, by using $\sqrt{(\sigma_{A,i}^2 + \sigma_{B,i}^2)}$. Simulations showed that the results from linear fitting were similar to those from the non-linear algorithms described by Verveer & Bastiaens (2003), even for data distorted by substantial amounts of Poisson noise (results not shown).

An example of cellular FLIM data is given in Fig. 1(b), where we plot the ($A_i$, $B_i$) pairs for data acquired from MCF7 cells expressing EGFP fused to epidermal growth factor receptor (EGFR-GFP, Wouters & Bastiaens, 1999). These cells were stimulated with epidermal growth factor and then fixed and incubated with a Cy3-labelled antibody against phosphotyrosine (PY72-Cy3, for more information about the assay and applications, see Verveer *et al.*, 2000b). The two components in this system are the unphosphorylated receptor, with the normal fluorescence decay for EGFP, and the phosphorylated receptor, with a faster fluorescence decay due to the occurrence of FRET between EGFP and Cy3. As expected for a mixture of two components the data lie on a straight line (closed circles). We applied a linear fit, without error weighing, to the data of Fig. 1(b). Subsequent calculation of the lifetimes of EGFR-GFP in its unphosphorylated and phosphorylated states via Eq. (3) yielded values of 2.23 and 0.72 ns. The values found by the global algorithm described by Verveer & Bastiaens (2003), which minimizes Eq. (5), were 2.22 and 0.69 ns. These values are comparable to those found earlier using much larger data sets (Verveer *et al.*, 2000b; Verveer & Bastiaens, 2003). Thus, the linear estimation approach appears to work well, in spite of a lack of proper error weighting.

To get a feel for the behaviour of a mixture of mono-exponential components, we simulated a mixture with lifetimes equal to the measured values of 2.23 and 0.72 ns. The $\alpha_i$ were chosen from a normal distribution with a mean of 0.7 and a standard deviation of 0.2, rejecting values below zero and above one. FLIM data were then simulated and Poisson noise was added. The level of noise is determined by the mean of the simulated data. This mean was chosen such that in simulations of a single component with a lifetime of 2.23 ns, the standard deviation of the estimated phase lifetime was equal to 0.12 ns. This value is in the range to be expected for data taken with a current single-frequency FLIM instrument (Hanley *et al.*, 2001; Verveer *et al.*, 2001b). From the simulated data, the $A$ and $B$ values were estimated and plotted (Fig. 1b, open circles). The measured and simulated data show similar noise properties, suggesting that a two-component model describes the data well.

### Mixtures of two components with a complex pure component decay

Our discussion has thus far concentrated on the situation of a two-component system with each component having a unique but single exponential decay time. In general, any two-component model can be represented as a linear set of equations:

$$A_i = M_i\sin(\varphi_i) = \alpha_i M_1\sin(\varphi_1) + (1 - \alpha_i)M_2\sin(\varphi_2), \qquad (6a)$$

$$B_i = M_i\cos(\varphi_i) = \alpha_i M_1\cos(\varphi_1) + (1 - \alpha_i)M_2\cos(\varphi_2), \qquad (6b)$$

where the spatially invariant phase ($\varphi_1$, $\varphi_2$) and modulation values ($M_1$, $M_2$) represent the pure component fluorescence decays, which are not necessarily single-exponential. This formulation illustrates the general utility of this representation of frequency-domain lifetime data even in cases where the individual components each have complex (non-exponential) decay laws. In the latter situation a plot of $A$ vs. $B$ should still yield a straight line. However, its endpoints will not lie on the half-circle of single-exponential components and a fit assuming single-exponentials will therefore lead to a rescaling of the population values. It should be noted that the sensitivity with which a fluorescent decay component is detected depends on the measurement frequency (Gadella *et al.*, 1993, 1994). Thus, a fluorescence species may appear less or more homogeneous in single-frequency FLIM data, depending on the frequency

chosen. Consequently, the model error that is introduced by heterogeneity may be minimized by a judicious choice of the measurement frequency.

EGFP is known generally to exhibit more than a single exponential in its decay (Pepperkok *et al.*, 1999; Uskova *et al.*, 2000). Indeed, phase and modulation lifetime values measured from a fixed sample with EGFR-GFP alone were reported to be slightly different, indicating some heterogeneity in the fluorescence decay (Verveer *et al.*, 2001b). In addition, the short lifetime component in samples exhibiting FRET may show heterogeneity due to the fact that more than one Cy3 molecule may be attached to each antibody, leading to multiple paths for energy transfer with different rates. A thorough analysis of such an FRET pair requires high-resolution measurements on pure samples. This is difficult to achieve with single-frequency instrumentation and with cellular samples exhibiting population heterogeneity. The EGFR-GFP/PY72-Cy3 system has been validated in biological systems: in earlier work Verveer *et al.* (2001b) analysed FLIM data acquired at 80 MHz and concluded that at the plasma membrane EGFR-receptors were all phosphorylated ($\alpha = 1$) and not elsewhere after stimulation with saturating levels of epidermal growth factor, as is expected. It thus appears that, in this system, heterogeneity in the fluorescence decays of the individual components does not play a significant role in practical biological applications.

### Tertiary and higher-order mixtures

The model presented here can be easily generalized to higher-order mixing of components. The $(A, B)$ plot of an $N$-component mixture will be bounded by a polygon containing $N$-vertices. For pure single lifetime components these vertices will intersect with the semicircle defining single exponential decays. A more detailed analysis of these situations including noise and non-exponential decays is beyond the scope of this short communication. For the present data set it is conceivable that the band of data-points could also be modelled as a polygon-area with multiple intersection points with half-circle of single exponential lifetimes. However, the simulations shown in Fig. 1(b) corroborate that the two-state model is adequate in this case.

### Conclusions

We have demonstrated a graphical method that allows the estimation of the lifetimes of a two-component model from single-frequency FLIM data and hence can be used to obtain component population maps in living cells. Importantly, this shows that, given sufficient variation in populations, it is indeed possible to find unambiguously the two pure-component lifetimes, validating the use of global analysis methods to resolve a two-component model with single-frequency FLIM data. Furthermore, we have described a linear estimation method that from simulations and application to real data appears to perform similar to non-linear global analysis methods that account for the noise properly. We have briefly touched upon the subject of dealing with mixtures of components with heterogeneous decays. Real-world data are likely to show at least some degree of heterogeneity, and therefore this type of analysis should be applied with care. In the case of the EGFR-GFP/PY72-Cy3 system discussed here, the simple two-component model with single-exponential decay laws is adequate for most biological applications. We are currently investigating the quantitative analysis of single-frequency FLIM data in terms of models with more complex decay laws.

### Acknowledgement

A.H.A.C. is the recipient of a Long-term Fellowship from the Human Frontier Science Program Organization.

### References

Bastiaens, P.I.H. & Squire, A. (1999) Fluorescence lifetime imaging microscopy: spatial resolution of biochemical processes in the cell. *Trends Cell Biol.* **9**, 48–52.

Gadella, T.W.J. Jr, Clegg, R.M. & Jovin, T.M. (1994) Fluorescence lifetime imaging microscopy: pixel-by-pixel analysis of phase-modulation data. *Bioimaging*, **2**, 139–159.

Gadella, T.W.J. Jr, Jovin, T.M. & Clegg, R.M. (1993) Fluorescence lifetime imaging microscopy (FLIM) – spatial resolution of microstructures on the nanosecond time-scale. *Biophys. Chem.* **48**, 221–239.

Hanley, Q.S., Subramaniam, V., Arndt-Jovin, D.J. & Jovin, T.M. (2001) Fluorescence lifetime imaging: multi-point calibration, minimum resolvable differences, and artifact suppression. *Cytometry*, **43**, 248–260.

Hirshfield, K.M., Toptygin, D., Packard, B.S. & Brand, L. (1993) Dynamic fluorescence measurements of 2-state systems – applications to calcium-chelating probes. *Anal. Biochem.* **209**, 209–218.

Itagaki, M., Honoso, M. & Watanabe, K. (1997) Analysis of pyrene fluorescence emission by fast Fourier transformation. *Anal. Sci.* **13**, 991–996.

Lakowicz, J.R. & Berndt, K. (1991) Lifetime-selective fluorescence imaging using an rf phase-sensitive camera. *Rev. Sci. Instrum.* **62**, 1727–1734.

Lakowicz, J.R., Jayaweera, R., Joshi, N. & Gryczynski, I. (1987) Correction for contaminant fluorescence in frequency-domain fluorometry. *Anal. Biochem.* **160**, 471–479.

Pepperkok, R., Squire, A., Geley, S. & Bastiaens, P.I.H. (1999) Simultaneous detection of multiple green fluorescent proteins in live cells by fluorescence lifetime imaging microscopy. *Curr. Biol.* **9**, 269–272.

Press, W.H., Teukolsky, S.A., Vetterling, W.T. & Flannery, B.P. (1992) *Numerical Recipes in C*. Cambridge University Press, Cambridge, U.K.

Uskova, M.A., Borst, J.-W.H., Ink, M.A., van Hoek, A., Schots, A., Klyachko, N.L. & Visser, A.J.W.G. (2000) Fluorescence dynamics of green fluorescent protein in AOT reversed micelles. *Biophys. Chem.* **87**, 73–84.

Verveer, P.J. & Bastiaens, P.I.H. (2003) Evaluation of global analysis algorithms for single frequency fluorescence lifetime imaging microscopy data. *J. Microsc.* **209**, 1–7.

Verveer, P.J., Squire, A. & Bastiaens, P.I.H. (2000a) Global analysis of fluorescence lifetime imaging microscopy data. *Biophys. J.* **78**, 2127–2137.

Verveer, P.J., Squire, A. & Bastiaens, P.I.H. (2001a) Frequency-domain fluorescence lifetime imaging microscopy: a window on the biochemical landscape of the cell. *Methods in Cellular Imaging* (ed. by A. Periasamy), pp. 273–292. Oxford University Press, Oxford.

Verveer, P.J., Squire, A. & Bastiaens, P.I.H. (2001b) Improved spatial discrimination of protein reaction states in cells by global analysis and deconvolution of fluorescence lifetime imaging microscopy data. *J. Microsc.* **202**, 451–456.

Verveer, P.J., Wouters, F.S., Reynolds, A.R. & Bastiaens, P.I.H. (2000b) Quantitative imaging of lateral ErbB1 receptor signal propagation in the plasma membrane. *Science*, **290**, 1567–1570.

Weber, G. (1981) Resolution of the fluorescence lifetimes in a heterogeneous system by phase and modulation measurements. *J. Phys. Chem.* **85**, 949–953.

Wouters, F.S. & Bastiaens, P.I.H. (1999) Fluorescence lifetime imaging of receptor tyrosine kinase activity in cells. *Curr. Biol.* **9**, 1127–1130.

Wouters, F.S., Verveer, P.J. & Bastiaens, P.I.H. (2001) Imaging biochemistry inside cells. *Trends Cell Biol.* **11**, 203–211.